Structure determination of multicomponent crystalline phases of (*S*)-ibuprofen and L-proline from powder X-ray diffraction data, augmented by complementary experimental and computational techniques

Okba Al Rahal, P. Andrew Williams, Colan E. Hughes, Benson M. Kariuki, Kenneth D. M. Harris*

School of Chemistry, Cardiff University, Park Place, Cardiff CF10 3AT, Wales, U. K.

* Author for correspondence: HarrisKDM@cardiff.ac.uk

Abstract

Two multicomponent crystalline phases of (*S*)-ibuprofen and L-proline with 1:1 stoichiometry are reported, specifically a non-solvate phase (**Ibu-Pro)** and a quarter-hydrate phase (**Ibu-Pro-QH**). **Ibu-Pro** was prepared only by solid-state mechanochemical synthesis, while **Ibu-Pro-QH** was obtained both by solution-state crystallization and by solid-state mechanochemistry. The crystal structures of **Ibu-Pro** and **Ibu-Pro-QH** were determined directly from powder X-ray diffraction (XRD) data, with structure solution carried out using the direct-space strategy (implemented with a genetic algorithm search procedure) and structure refinement carried out using the Rietveld method. The process of structure determination from powder XRD data was augmented by information from other complementary techniques, specifically solid-state NMR spectroscopy, thermal analysis methods and periodic DFT-D calculations. A preliminary powder XRD study of the dehydration behaviour of **Ibu-Pro-QH** at elevated temperature is also reported.

Keywords

Multicomponent crystal, ibuprofen, proline, direct-space structure solution, powder XRD, solid-state NMR

1. Introduction

In the development of organic crystalline solids for materials applications, the pure crystalline phase of the active component is often unsuitable as a consequence of structural features and/or physico-chemical properties that are non-optimal for the required application. For example, in the case of pharmaceutically active molecules, the pure crystalline phase may have low solubility and/or low dissolution rate, which could be detrimental in pharmaceutical applications on account of the consequences of these properties for bioavailability. One strategy[1-11] to enhance the physicochemical properties of crystalline phases for such applications is to prepare multicomponent crystalline materials containing the active component together with one or more other types of molecule (we use the term "multicomponent crystal" as a general descriptor of any crystalline material that contains two or more different types of molecule,[12] encompassing materials that are variously described as co-crystals, inclusion compounds, solvates, hydrates, etc.). Although the formation of multicomponent crystals is not necessarily predictable (as the formation mechanism and relative stability may depend on the interplay of several kinetic and thermodynamic factors), a range of strategies may be used to explore the phase space available to the system, including different procedures for materials preparation (e.g., crystallization from solution or mechanochemical techniques) coupled with robust methods for structural characterization. When it is not feasible to obtain a single-crystal specimen of suitable size and quality for structural characterization by single-crystal X-ray diffraction (XRD), structure determination must be tackled instead using powder XRD data. Although structure determination from powder XRD data is more challenging than from single-crystal XRD data, modern methodology[13-19] allows crystal structures of organic molecular materials of moderate complexity to be determined from powder XRD, particularly by exploiting the direct-space strategy for structure solution and the Rietveld method for structure refinement. Furthermore, the process of structure determination from powder XRD data may be enhanced[20-22] by taking advantage of insights gained from complementary experimental (e.g., solid-state NMR) and computational (e.g., periodic DFT-D) techniques. Such multi-technique approaches are particularly advantageous in tackling challenging structure-determination problems, such as complex multicomponent structures defined by a significant number of structural variables.

Here we report two new multicomponent crystalline phases containing (*S*)-ibuprofen (Figure 1a) and L-proline (Figure 1b) with 1:1 stoichiometry, denoted **Ibu-Pro** (a non-solvate phase) and **Ibu-Pro-QH** (a quarter-hydrate phase). We note that (*S*)-ibuprofen is widely used in pharmaceutical applications due to its analgesic properties, and is the biologically active enantiomer of ibuprofen in humans [the (*R*)-enantiomer is not biologically active, but is converted enzymatically to the active

(*S*)-enantiomer in the human body]. **Ibu-Pro** was prepared only by solid-state mechanochemical synthesis,[23-25] while **Ibu-Pro-QH** was obtained both by crystallization from solution and by solid-state mechanochemistry. Structural characterization of both materials was carried out from powder XRD data, revealing interesting similarities and differences in their structural properties. Preliminary studies of the dehydration behaviour of **Ibu-Pro-QH** at elevated temperature are also reported. We note that several multicomponent crystalline materials containing ibuprofen[26-33] or L-proline[34] together with other molecules have been reported previously.

2. Experimental

(*S*)-ibuprofen was purchased from Aldrich and L-proline was purchased from Alfa Aesar.

Ibu-Pro was prepared by liquid-assisted milling[24] using a MM400 Retsch ball mill. One drop of methanol was added to a physical mixture of powder samples of (*S*)-ibuprofen and L-proline in 1:1 molar ratio. The mixture was placed inside a milling jar (volume, 1.5 ml) containing four stainless steel balls (diameter, 3.18 mm), with milling carried out at 30 Hz for 30 min. **Ibu-Pro** was obtained only the first time this experimental procedure was carried out. Repeated experiments using the same procedure as well as variants of this procedure (see details below), including dry milling or liquid-assisted milling with different liquids and/or different amounts of liquid, instead produced materials that were identified from powder XRD as **Ibu-Pro-QH**.

Ibu-Pro-QH was prepared by slow evaporation of solvent (ethanol, water/ethanol or water) from solutions containing a 1:1 molar ratio of (*S*)-ibuprofen and L-proline. The general procedure involved heating the solution to *ca.* 40 °C to achieve complete dissolution, followed by cooling to ambient temperature and then maintaining the solution at ambient temperature to allow slow evaporation. Under all sets of conditions, the microcrystalline powder collected after a few days gave the powder XRD pattern characteristic of **Ibu-Pro-QH**.[35] As stated above, **Ibu-Pro-QH** was also obtained under a range of different milling conditions, in particular using dry milling and liquid-assisted milling for different milling times (20 or 30 min) as well as using different liquids (methanol, ethanol, water) and different amounts of liquid (ranging from one drop to a few drops) in the liquid-assisted milling experiments.

For structure determination, high-quality powder XRD data were recorded at 21 °C on a Bruker D8 instrument (Ge-monochromated Cu$K\alpha_1$ radiation) operating in transmission mode. The powder

sample was packed into three glass capillaries, which were then sealed and attached to the disc sample holder of the powder XRD instrument (2θ range, 3.5° – 70°; step size, 0.017°; data collection time, 17 hr for **Ibu-Pro**, 64 hr for **Ibu-Pro-QH**).

Dehydration of **Ibu-Pro-QH** was studied by *in-situ* powder XRD on beamline I11 at Diamond Light Source. The powder sample was packed in a glass capillary (diameter, 0.7 mm), which was sealed by vacuum grease. Initially, a powder XRD pattern was recorded at ambient temperature using a multi-analyser-crystal (MAC) detector (λ = 0.82659 Å; 2θ range, 1° – 150°; step size, 0.004°; total time, 15 min). The capillary was then opened by removing the vacuum grease and the sample was heated to 77 °C using an Oxford CryoStream System. Powder XRD data were recorded at 77 °C as a function of time for 10 min at intervals of 1 min using a position-sensitive (PSD) detector (λ = 0.82652 Å; 2θ range, 1° – 92°; step size, 0.004°; time to record each powder XRD pattern, *ca*. 1 s). After the sample had been at 77 °C for 10 min, a final powder XRD pattern was recorded using the MAC detector (with the same data collection parameters described above for the MAC detector at ambient temperature).

Liquid-state ^{1}H NMR data were recorded on a Bruker AVANCE III HD NMR spectrometer (^{1}H Larmor frequency, 400 MHz) for a sample of **Ibu-Pro-QH** dissolved in methanol-d_4 (16 scans; time per scan, 10 s).

High-resolution solid-state ^{13}C NMR data were recorded for **Ibu-Pro-QH** using a Bruker AVANCE III spectrometer at the UK 850 MHz Solid-State NMR Facility (^{13}C Larmor frequency, 213.82 MHz; 4 mm HXY probe in double-resonance mode; zirconia rotor; 20 °C). The ^{13}C NMR spectra were recorded using ramped ^{1}H→^{13}C cross-polarization[36] together with ^{1}H decoupling using SPINAL-64[37] and magic-angle spinning (MAS) at two frequencies (11 kHz and 12 kHz) to facilitate the assignment of spinning sidebands.

Thermogravimetric Analysis (TGA) was carried out on polycrystalline samples of **Ibu-Pro** and **Ibu-Pro-QH** using a 4000 TGA (Perkin Elmer) instrument, with the sample (initial mass *ca*. 10 – 20 mg) in an aluminium pan. The TGA data were recorded on heating the sample at 5 °C/min from ambient temperature to 300 °C (**Ibu-Pro**) or 200 °C (**Ibu-Pro-QH**).

Periodic density functional theory (DFT-D) calculations were carried out using CASTEP[38] (Academic Release version 8.0). The calculations used ultrasoft pseudopotentials,[39] the PBE

functional,[40] semi-empirical dispersion corrections using the TS correction scheme,[41] fixed unit cell, preserved space group symmetry, periodic boundary conditions, a basis set cut-off energy of 700 eV and a Monkhorst-Pack grid[42] of minimum sample spacing ($0.05 \times 2\pi$) $Å^{-1}$. The convergence criteria for geometry optimization were 0.01 eV $Å^{-1}$ for forces, 0.00001 eV per atom for energy and 0.001 Å for atomic displacements.

3. Results and Discussion

3.1 *Thermal Analysis*

TGA data for **Ibu-Pro** (Figure S1; Supporting Information) show no mass loss below the melting temperature (122 °C), consistent with the assignment of **Ibu-Pro** as a non-solvate (anhydrous) material. After melting, a significant mass loss, attributed to decomposition, occurs above *ca*. 130 °C.

In the TGA data recorded for **Ibu-Pro-QH** on heating (Figure S2), a mass loss step of *ca*. 1.33% is observed from just above ambient temperature to *ca*. 100 °C. As **Ibu-Pro-QH** was prepared under a range of different conditions (including solution-state crystallization using different solvents as well as dry milling and liquid-assisted milling using different liquids), the only "solvent" to which the material was exposed under all preparation conditions was water (either from the crystallization solvents, the liquid drops used in liquid-assisted milling, or from the atmosphere). Thus, the only plausible interpretation for the mass loss observed in the TGA data is that **Ibu-Pro-QH** is a hydrate phase, as confirmed subsequently by crystal structure determination (Section 3.4). The mass loss in the TGA data is therefore assigned to dehydration. As discussed in Section 3.2, liquid-state ^{1}H NMR data confirms that **Ibu-Pro-QH** contains (*S*)-ibuprofen and L-proline in 1:1 molar ratio; on this basis, the mass loss of 1.33% corresponds to one quarter equivalent of water (theoretical mass loss, 1.38%).

3.2 *Liquid-State ^{1}H NMR and Solid-State ^{13}C NMR*

To determine the molar ratio of (*S*)-ibuprofen and L-proline in **Ibu-Pro-QH**, the liquid-state ^{1}H NMR spectrum (Figure S3) was recorded for a solution prepared by dissolving **Ibu-Pro-QH** in methanol-d_4. The liquid-state ^{1}H NMR spectrum confirms that **Ibu-Pro-QH** contains (*S*)-ibuprofen and L-proline in 1:1 molar ratio (see Section S2 for more details).

High-resolution solid-state ^{13}C NMR data for **Ibu-Pro-QH** were used in conjunction with structure determination from powder XRD data to provide an independent assessment of the number

of molecules in the asymmetric unit. In the solid-state ^{13}C NMR spectrum (Figure S4), two peaks with isotropic chemical shifts in the region of 60 ppm (and with approximately equal intensities) are assigned to the C(β) environment of L-proline, indicating that there are two independent molecules of L-proline in the asymmetric unit. As it is known from liquid-state ^{1}H NMR that (*S*)-ibuprofen and L-proline are present in 1:1 molar ratio, it follows that **Ibu-Pro-QH** also contains two independent molecules of (*S*)-ibuprofen in the asymmetric unit.[43] As we have determined from TGA data that **Ibu-Pro-QH** contains one quarter equivalent of water, we deduce that there is one half molecule of water in the asymmetric unit.

As only a limited amount of **Ibu-Pro** was obtained in our work, it was not feasible to record liquid-state ^{1}H NMR data or solid-state ^{13}C NMR data for this material.

3.3 *Structure Determination of Ibu-Pro from Powder XRD Data*

Ibu-Pro was obtained by solid-state mechanochemical synthesis as a microcrystalline powder, and thus structure determination from powder XRD data provides the most viable route to structural characterization.[44-49] The powder XRD pattern of **Ibu-Pro** was indexed using the program TREOR[50] in the CRYSFIRE package,[51] giving the following unit cell with monoclinic metric symmetry: a = 14.43 Å, b = 5.81 Å, c = 21.81 Å, β = 97.10°, V = 1814 Å^3. As **Ibu-Pro** contains single enantiomers of (*S*)-ibuprofen and L-proline, the space group must be chiral (P2, P2$_1$ or C2). Space group C2 was ruled out on the basis of systematic absences. To establish whether the correct space group is P2 or P2$_1$, structure solution calculations were carried out for both space groups.

Profile fitting using the Le Bail method[52] in the GSAS program[53] gave a good-quality fit to the powder XRD data, as shown (for space group P2$_1$) in Figure 2a (R_{wp} = 3.11%, R_p = 2.33%).

Structure solution was carried out independently for space groups P2 and P2$_1$ using the direct-space genetic algorithm (GA) technique in the program EAGER.[54-60] Density considerations suggest that the unit cell contains four molecules of (*S*)-ibuprofen and four molecules of L-proline, corresponding to two molecules of (*S*)-ibuprofen and two molecules of L-proline in the asymmetric unit for either space group P2 or P2$_1$.

In the GA structure-solution calculations, each (*S*)-ibuprofen molecule was defined by ten structural variables (three positional, three orientational and four torsional variables) and each L-

proline molecule was defined by seven structural variables (three positional, three orientational and one torsional variables). The ring conformation in the L-proline molecules was taken from the reported crystal structure of L-proline[61] (REF Code: PROLIN) and was fixed in the structure solution calculations.[62] The *y*-coordinate of one L-proline molecule was fixed (for space groups P2 and $P2_1$, the position of one molecule may be fixed along the *b*-axis). Thus, the total number of structural variables in the GA structure-solution calculation was 33. For each space group, the GA calculations involved the evolution of a population of 500 trial structures for 600 generations, with 50 mating operations and 250 mutation operations per generation. In total, 16 independent GA structure-solution calculations were carried out in parallel.

The structure-solution calculations for space group $P2_1$ produced structures that are chemically and structurally sensible, and give a good fit to the experimental powder XRD data. However, no reasonable structure solutions were obtained for space group P2, which was not considered further. Four of the 16 independent GA calculations for space group $P2_1$ produced the same structure solution giving the best fit (i.e., lowest R_{wp}) to the experimental powder XRD data, which was used as the initial structural model for Rietveld refinement.

In the Rietveld refinement, standard restraints were applied to bond lengths and bond angles (based on geometric information from MOGUL[63] and, for bonds involving hydrogen, from Allen *et al.*[64]). Planar restraints were applied to the carboxylic acid group of (*S*)-ibuprofen, the carboxylate group of L-proline and the aromatic ring of (*S*)-ibuprofen. A common isotropic displacement parameter was refined for the non-hydrogen atoms of the two molecules of (*S*)-ibuprofen and a common isotropic displacement parameter was refined for the non-hydrogen atoms of the two molecules of L-proline. The isotropic displacement parameter for hydrogen atoms was set as 1.2 times that for the non-hydrogen atoms in the same molecule. At various stages during Rietveld refinement, the structure was subjected to DFT-D geometry optimization (with fixed unit cell) in order to check that the structure is close to an energy minimum and to improve aspects of molecular geometry (for example, the ring conformation of the L-proline molecules). The geometric restraints in the Rietveld refinement were updated to match the molecular geometries obtained in the DFT-D calculations.

The final Rietveld refinement gave a good-quality fit between calculated and experimental powder XRD data (R_{wp} = 3.45%, R_p = 2.51%; Figure 2b), comparable to the quality of fit obtained in

profile-fitting (R_{wp} = 3.11%, R_p = 2.33%; Figure 2a); final refined lattice parameters: a = 14.42962(32) Å, b = 5.80927(14) Å, c = 21.8184(9) Å, β = 97.1140(24)°, V = 1814.86(11) Å^3.

The final refined structure was subjected to geometry optimization (with fixed unit cell) using periodic DFT-D calculations. The geometry-optimized structure shows only minor differences in atom positions compared to the structure from Rietveld refinement (RMSD = 0.19 Å for non-hydrogen atoms), confirming that the final refined structure is very close to an energy minimum. The structure from Rietveld refinement and the geometry-optimized structure are compared in Figure S5.

3.4 *Structure Determination of Ibu-Pro-QH from Powder XRD Data*

The powder XRD pattern of **Ibu-Pro-QH** was indexed using the program FJZN in the CRYSFIRE package, giving the following unit cell with monoclinic metric symmetry: a = 33.11 Å, b = 5.69 Å, c = 20.29 Å, β = 100.85°, V = 3760 Å^3. On the basis of systematic absences and recognizing that the structure must be chiral, the space group was assigned as C2. Profile fitting for space group C2 using the Le Bail method in the GSAS program gave a good-quality fit to the experimental powder XRD data (R_{wp} = 1.84%, R_p = 1.37%; Figure 3a).

Structure solution of **Ibu-Pro-QH** was carried out using the direct-space GA technique in the program EAGER. Density considerations suggest that the unit cell contains eight molecules of (*S*)-ibuprofen and eight molecules of L-proline. As space group C2 has a multiplicity of 4, the asymmetric unit must comprise two molecules of (*S*)-ibuprofen and two molecules of L-proline, consistent with the assignment from solid-state ^{13}C NMR data discussed in Section 3.2. In addition, the material contains one quarter equivalent of water (see Section 3.1), corresponding to one half molecule of water in the asymmetric unit. For space group C2, the half molecule of water must lie on a crystallographic 2-fold rotation axis, with the molecular 2-fold axis coincident with the crystallographic 2-fold axis.

For the GA structure-solution calculations, the (*S*)-ibuprofen and L-proline molecules were constructed as described for **Ibu-Pro** in Section 3.3. The *y*-coordinate of one L-proline molecule was fixed (for space group C2, the position of one molecule may be fixed along the *b*-axis). The half molecule of water was represented by a single oxygen atom located on the crystallographic 2-fold axis, defined by one structural variable (position along the 2-fold axis). In total, the number of structural variables in the GA structure solution calculation was 34. The GA calculations involved

the evolution of a population of 500 trial structures for 500 generations, with 50 mating operations and 250 mutation operations per generation. In total, 16 independent GA calculations were carried out in parallel.

Four of the 16 independent GA structure-solution calculations generated essentially the same structure giving the best fit to the experimental powder XRD data (i.e., lowest R_{wp}). This structure was used as the initial model for Rietveld refinement, which was carried out using the general strategy[65] described for **Ibu-Pro** in Section 3.3. The initial Rietveld refinement gave a good-quality fit between calculated and experimental powder XRD data (R_{wp} = 2.93%, R_p = 2.11%), although the structure contained an unfavourable short contact between an L-proline molecule and an (*S*)-ibuprofen molecule. This issue was resolved by carrying out a DFT-D geometry-optimization calculation (with fixed unit cell), which alleviated the unfavourable short contact and gave a geometrically reasonable hydrogen-bonding scheme. The structure from DFT-D geometry optimization was then used as the starting structure in further Rietveld refinement, which gave an improved fit to the experimental powder XRD data (Figure 3b; R_{wp} = 2.57%, R_p = 1.82%), comparable to the quality of fit obtained in profile-fitting (Figure 3a); final refined lattice parameters: a = 33.1379(14) Å, b = 5.69453(19) Å, c = 20.2919(7) Å, β = 100.8658(31)°, V = 3760.5(2) Å^3.

The final refined structure was subjected to geometry optimization (with fixed unit cell) using periodic DFT-D calculations. The geometry-optimized structure shows only small differences in atom positions compared to the structure from Rietveld refinement (RMSD = 0.29 Å for non-hydrogen atoms), confirming that the final refined structure is close to an energy minimum. The structure determined from Rietveld refinement and the geometry-optimized structure are compared in Figure S6 (the largest discrepancy concerns a small difference in the conformation of the iso-propyl group of one of the two independent (*S*)-ibuprofen molecules, with no significant discrepancies in the hydrogen-bonding arrangement).

3.5 *Structural Properties of Ibu-Pro*

The crystal structure of **Ibu-Pro** (Figure 4) contains an extended hydrogen-bonding arrangement involving the two independent L-proline molecules (labelled A and B in Figure 4) and the symmetry-related L-proline molecules generated by the 2_1-screw axis (labelled A' and B' in Figure 4). The L-proline molecules labelled A are linked through hydrogen bonding both to the symmetry-related A'

molecules (giving rise to hydrogen-bonded A-A' ribbons running parallel to the *b*-axis) and to the independent B molecules (giving rise to hydrogen-bonded A-B ribbons that also run parallel to the *b*-axis). The (*S*)-ibuprofen molecules are linked through a single hydrogen bond to the periphery of the hydrogen-bonded ribbons of L-proline molecules. As shown in Figure S7, the two independent (*S*)-ibuprofen molecules have similar conformations, while the two independent L-proline molecules exhibit slight differences in ring conformation.

The A-A' ribbons (Figure 5a) are constructed from two strands of L-proline molecules running along the *b*-axis, with the two strands related to each other by the 2_1-screw axis. Within a given strand, adjacent L-proline molecules are related by translation along the *b*-axis and are linked by an N–H···O hydrogen bond between the ammonium group (N–H donor) of one molecule and the carboxylate group (O acceptor) of the adjacent molecule. The two strands of the ribbon are cross-linked by an N–H···O interaction that deviates significantly from linearity (N···O, 2.78 Å; N–H···O, 129°) between an ammonium group (N–H donor) in one strand and a carboxylate group (O acceptor) in the other strand. Each L-proline molecule is engaged in two (symmetry-related) cross-linking N–H···O hydrogen bonds of this type, in one case as N–H donor and in the other case as O acceptor, involving two different L-proline molecules in the other strand.

The A-B ribbons (Figure 5b) are constructed from two strands of L-proline molecules running along the *b*-axis, with no symmetry relation between the two strands. Adjacent L-proline molecules in a given strand are related by translation along the *b*-axis and are linked by N–H···O hydrogen bonds between an ammonium group (N–H donor) and a carboxylate group (O acceptor). The two strands in the ribbon are cross-linked by an N–H···O hydrogen bond involving an ammonium group in the B strand (N–H donor) and a carboxylate group (O acceptor) in the A strand; each molecule is engaged in one interaction of this type. The corresponding N–H donor of the ammonium group in the A strand is involved in a cross-linking N–H···O hydrogen bond within the A-A' ribbon, as discussed above.

The (*S*)-ibuprofen molecules are arranged along the periphery of the ribbons of L-proline molecules (Figure 4). Each (*S*)-ibuprofen molecule forms an O–H···O hydrogen bond with an L-proline molecule, involving the carboxylic acid group of (*S*)-ibuprofen (O–H donor) and the carboxylate group of L-proline (O acceptor). In each case, the C–O bond of the L-proline molecule involved in this O–H···O hydrogen bond with (*S*)-ibuprofen is the C–O bond that acts as acceptor in

the N–H···O hydrogen bond between adjacent molecules within the strand along the *b*-axis (for the A strand, this C–O bond is also involved in N–H···O cross-linking to the A' strand in the A-A' ribbon; for the B strand, this C–O bond is not involved in any N–H···O cross-linking to the A strand in the A-B ribbon). For each (*S*)-ibuprofen molecule, the C=O bond of the carboxylic acid group is not engaged in any hydrogen bonding.

3.6 *Structural Properties of Ibu-Pro-QH*

The crystal structure of **Ibu-Pro-QH** (Figure 6) is described in terms of two hydrogen-bonded regions: one region contains the water molecules (denoted region W; enclosed by the blue dotted line in Figure 6) and the other region does not contain water molecules (denoted region N; enclosed by the red dotted line in Figure 6). The asymmetric unit comprises two independent molecules of (*S*)-ibuprofen (one in region N and one in region W), two independent molecules of L-proline (one in region N and one in region W) and one half molecule of water (in region W). The two independent (*S*)-ibuprofen molecules have significantly different conformations (Figure S8a) and the two independent molecules of L-proline also exhibit differences in ring conformation (Figure S8b).

Region N of **Ibu-Pro-QH** contains a hydrogen-bonded ribbon of L-proline molecules running along the *b*-axis (Figure 7a), constructed from two strands of L-proline molecules that are related to each other by the 2_1-screw axis parallel to the *b*-axis. Within a given strand of this ribbon, adjacent L-proline molecules are related by translation along the *b*-axis and are linked by an N–H···O hydrogen bond between the ammonium (N–H donor) and carboxylate (O acceptor) groups (see Figure 7a); the same N–H donor is also involved in a rather long and non-linear N–H···O interaction with the other oxygen atom of the carboxylate group; however, based on geometric criteria (N···O, 3.32 Å; N–H···O, 132°), this interaction may not be significant. The molecules in different strands are cross-linked by N–H···O hydrogen bonds; each L-proline molecule is engaged in two (symmetry-related) cross-linking N–H···O hydrogen bonds of this type, in one case as N–H donor and in the other case as O acceptor, involving two different L-proline molecules in the other strand. Clearly, the hydrogen-bonded ribbons of L-proline molecules in region N of **Ibu-Pro-QH** (Figure 7a) share several structural similarities to the A-A' ribbons of L-proline molecules in **Ibu-Pro** (Figure 5a). The (*S*)-ibuprofen molecules in region N are located at each edge of the ribbon. Each (*S*)-ibuprofen molecule forms an O–H···O hydrogen bond with an L-proline molecule in the ribbon, involving the carboxylic

acid group of (*S*)-ibuprofen as the O–H donor and an oxygen atom of the carboxylate group of L-proline as the acceptor (the same oxygen atom is also involved as acceptor in the N–H···O hydrogen bond between adjacent L-proline molecules within the strand along the *b*-axis). The C=O bond of the carboxylic acid group of the (*S*)-ibuprofen molecule is not engaged in hydrogen bonding.

In region W of **Ibu-Pro-QH**, the oxygen atom of the water molecule is located on a crystallographic 2-fold rotation axis parallel to the *b*-axis (Figure 6). The hydrogen-bonding in region W (Figure 7b) differs significantly from the hydrogen-bonding arrangements in region N and in **Ibu-Pro**. In region W, each O–H bond of the water molecule is engaged as the donor in an O–H···O hydrogen bond to the C=O bond of the carboxylic acid group of (*S*)-ibuprofen as the acceptor. The carboxylic acid group of (*S*)-ibuprofen is also engaged in two hydrogen bonds to a molecule of L-proline, specifically: (i) an O–H···O hydrogen bond involving the O–H bond of (*S*)-ibuprofen as the donor and the C–O bond of the carboxylate group of L-proline as the acceptor, and (ii) an N–H···O hydrogen bond involving an N–H bond of L-proline as the donor and the C=O bond of the carboxylic acid group of (*S*)-ibuprofen as the acceptor. Furthermore, the L-proline molecules in region W are arranged in hydrogen-bonded chains running along the *b*-axis. Adjacent molecules in this chain are related by translation along the *b*-axis and are linked by an N–H···O hydrogen bond. Clearly, the arrangement of molecules in region W has 2-fold symmetry. The water molecules are located on the 2-fold axis and are linked on each side to (*S*)-ibuprofen molecules, which in turn are linked to a chain of L-proline molecules.

3.7 *Preliminary Study of Dehydration of Ibu-Pro-QH*

Finally, we consider whether dehydration of **Ibu-Pro-QH** leads to formation of **Ibu-Pro**, assessed from a preliminary high-temperature powder XRD study. First, we recall that TGA experiments (Sections 3.1 and S1) show that mass loss occurs on heating **Ibu-Pro-QH**, consistent with complete loss of the quarter equivalent of water.

To explore the structural changes associated with this dehydration processes, *in-situ* high-temperature powder XRD studies were carried out on beamline I11 at Diamond Light Source. Figure S9 shows powder XRD patterns recorded: (i) at ambient temperature before heating **Ibu-Pro-QH** (Figure S9a), (ii) immediately after heating the sample from ambient temperature to 77 °C (Figure S9b), and (iii) after the sample had been at 77 °C for 10 min (Figure S9c).

First, we note that peaks characteristic of **Ibu-Pro** do not appear in the powder XRD pattern at any stage of this experiment, indicating that dehydration of **Ibu-Pro-QH** at 77 °C does not lead to formation of **Ibu-Pro** within the time period of our study. In particular, the diagnostic peak for **Ibu-Pro** at $2\theta \approx 7.47°$ (red dashed line in the simulated powder XRD pattern for **Ibu-Pro** in Figure S9d, calculated for $\lambda = 0.827$ Å) is clearly not observed in the experimental data.

From the powder XRD data recorded as a function of time at 77 °C, three observations are clear: (i) the sample remains predominantly as **Ibu-Pro-QH**, although the peak positions due to **Ibu-Pro-QH** shift gradually as a function of time, (ii) there is no evidence for the formation of **Ibu-Pro**, and (iii) soon after reaching 77 °C, some new low-intensity peaks appear in the powder XRD data and grow gradually in intensity as a function of time – however, by the end of the experiment, the intensity of these peaks is still significantly lower than the peaks due to **Ibu-Pro-QH**.

From TGA results (Section 3.1), **Ibu-Pro-QH** is known to undergo dehydration on heating above ambient temperature, suggesting that the predominant phase in the powder XRD study at 77 °C, giving rise to the powder XRD pattern characteristic of **Ibu-Pro-QH**, is a partially (or fully) dehydrated material that still retains the crystal structure of **Ibu-Pro-QH**. To rationalize the gradual shift in the peak positions for **Ibu-Pro-QH** as a function of time at 77 °C, the unit cell parameters were determined from Le Bail fitting of the powder XRD data, giving the variation in unit cell volume as a function of time shown in Figure S10. The initial unit cell volume of **Ibu-Pro-QH** at 77 °C is higher than the unit cell volume at ambient temperature (see Section 3.4) as a consequence of lattice expansion on heating.[66] From Figure S10, the unit cell volume then decreases monotonically with time at 77 °C, which may be attributed to relaxation of the structure of **Ibu-Pro-QH** following loss of water, but with no substantial structural changes. These observations suggest that dehydration of **Ibu-Pro-QH** is associated with only minor structural relaxation, giving a powder XRD pattern characteristic of **Ibu-Pro-QH** but with slight peak shifts indicative of a gradual decrease in unit cell volume as a function of time.

The new set of low-intensity peaks (two of which are highlighted in Figure S9c) that appear in the powder XRD data (alongside the significantly stronger peaks due to **Ibu-Pro-QH**) indicate that a small amount of a new crystalline phase emerges at 77 °C. As discussed above, this new phase is clearly <u>not</u> the **Ibu-Pro** phase. Given that the new phase represents only a minor component of the

sample in the final powder XRD data recorded at 77 °C, structure determination of this new phase has not been attempted. Future studies will aim to gain deeper insights into the dehydration process of **Ibu-Pro-QH**, including studies over significantly longer periods of time and at a wider range of temperatures, which may yield a monophasic sample of the new phase.

4. Concluding Remarks

The structural properties of non-solvate (**Ibu-Pro**) and quarter-hydrate (**Ibu-Pro-QH**) multicomponent crystalline phases containing (*S*)-ibuprofen and L-proline in 1:1 ratio have been determined directly from powder XRD data, with structure determination carried out using the direct-space GA strategy for structure solution followed by structure refinement using the Rietveld method. The hydration level of **Ibu-Pro-QH** was established both from thermal analysis (TGA) and from the crystal structure determination from powder XRD data. For both **Ibu-Pro** and **Ibu-Pro-QH**, the crystal structure contains one-dimensional ribbon-like hydrogen-bonded arrays of L-proline molecules, with the (*S*)-ibuprofen molecules linked by a single hydrogen bond to the periphery of these arrays. For **Ibu-Pro-QH**, another type of hydrogen-bonded array incorporates the water molecule, which is linked to a pair of (*S*)-ibuprofen molecules that are each engaged in hydrogen-bonding with a ribbon of L-proline molecules. Our preliminary high-temperature powder XRD study (at 77 °C) indicates that dehydration of **Ibu-Pro-QH** does not produce **Ibu-Pro**. Instead, **Ibu-Pro-QH** exhibits a slight decrease in unit cell volume as a function of time, consistent with a continuous dehydration process together with minor structural relaxation, which may suggest that the crystal structure of **Ibu-Pro-QH** can exist over a range of hydration levels. Furthermore, a small amount of a new crystalline phase is evident on dehydration of **Ibu-Pro-QH** at elevated temperature.

The crystal structures of **Ibu-Pro** and **Ibu-Pro-QH** reported here demonstrate the current opportunities for structure determination of complex organic materials from powder XRD data, particularly when analysis of the powder XRD data is augmented by insights from other experimental and computational techniques. We anticipate that multi-technique strategies of this type will facilitate the structure determination of even more complex multicomponent crystalline materials from powder XRD data in the future.

ASSOCIATED CONTENT

Supporting Information

The Supporting Information is available free of charge on the ACS Publications website at DOI: 10.1021/acs.cgd.????.

Thermal analysis (TGA) data for **Ibu-Pro** and **Ibu-Pro-QH**, liquid-state ^{1}H NMR data for **Ibu-Pro-QH**, solid-state ^{13}C NMR data for **Ibu-Pro-QH**, additional plots showing details of the structural properties of **Ibu-Pro** and **Ibu-Pro-QH**, and results from the preliminary high-temperature synchrotron powder XRD study of **Ibu-Pro-QH**.

Accession Codes

CCDC 2056854 – 2056855 contain the supplementary crystallographic data for this paper. These data can be obtained free of charge via www.ccdc.cam.ac.uk/data_request/cif, or by emailing data_request@ccdc.cam.ac.uk, or by contacting The Cambridge Crystallographic Data Centre, 12 Union Road, Cambridge CB2 1EZ, UK; fax: +44 1223 336033.

AUTHOR INFORMATION

Corresponding Author

*E-mail: HarrisKDM@cardiff.ac.uk

ORCID

Kenneth D. M. Harris: 0000-0001-7855-8598

Okba Al Rahal: 0000-0001-7553-9930

Benson M. Kariuki: 0000-0002-8658-3897

Notes

The authors declare no competing financial interest.

Acknowledgements

We are grateful to Cardiff University (PhD studentship to O. A. R.) and the Council for At-Risk Academics (Fellowship to O. A. R.) for support. We thank Diamond Light Source for beam-time on powder XRD beamline I11, Supercomputing Wales for access to computational facilities, and the U.K. High-Field Solid-State NMR Facility for the award of spectrometer time [this facility was funded by EPSRC and BBSRC (contract reference PR140003) as well as the University of Warwick,

including part funding through Birmingham Science City Advanced Materials Projects 1 and 2 supported by Advantage West Midlands and the European Regional Development Fund].

References

(1) Almarsson, Ö.; Zaworotko, M. J. Crystal engineering of the composition of pharmaceutical phases. Do pharmaceutical co-crystals represent a new path to improved medicines? *Chem. Commun.* **2004**, 1889-1896.

(2) Aakeröy, C. B.; Salmon, D. J. Building co-crystals with molecular sense and supramolecular sensibility. *CrystEngComm.* **2005**, *7*, 439-448.

(3) Trask, A.V.; Motherwell, W. D. S.; Jones, W. Pharmaceutical cocrystallization: Engineering a remedy for caffeine hydration. *Cryst. Growth Des.* **2005**, *5*, 1013-1021.

(4) Vishweshwar, P.; McMahon, J. A.; Bis, J. A.; Zaworotko, M. J. Pharmaceutical co-crystals. *J. Pharm. Sci.* **2006**, *95*, 499-516.

(5) Blagden, N.; de Matas, M.; Gavan, P. T.; York, P. Crystal engineering of active pharmaceutical ingredients to improve solubility and dissolution rates. *Adv. Drug. Delivery Rev.* **2007**, *59*, 617-630.

(6) Shan, N.; Zaworotko, M. J. The role of cocrystals in pharmaceutical science. *Drug Discovery Today* **2008**, *13*, 440-446.

(7) Schultheiss, N.; Newman, A. Pharmaceutical cocrystals and their physicochemical properties. *Cryst. Growth Des.* **2009**, *9*, 2950-2967.

(8) Good, D. J.; Rodriguez-Hornedo, N. Solubility advantage of pharmaceutical cocrystals. *Cryst. Growth Des.* **2009**, *9*, 2252-2264.

(9) Babu, N. J.; Nangia, A. Solubility advantage of amorphous drugs and pharmaceutical cocrystals. *Cryst. Growth Des.* **2011**, *11*, 2662-2679.

(10) Srirambhatla, V. K.; Kraft, A.; Watt, S.; Powell, A. V. Crystal design approaches for the synthesis of paracetamol co-crystals. *Cryst. Growth Des.* **2012**, *12*, 4870-4879.

(11) Duggirala, N. K.; Perry, M. L.; Almarsson, Ö.; Zaworotko, M. J. Pharmaceutical cocrystals: Along the path to improved medicines. *Chem. Commun.* **2016**, *52*, 640-655.

(12) Grothe, E.; Meekes, H.; Vlieg, E.; ter Horst, J. H.; de Gelder, R. Solvates, salts, and cocrystals: A proposal for a feasible classification system. *Cryst. Growth Des.* **2016**, *16*, 3237-3243.

(13) Lightfoot, P.; Tremayne, M.; Harris, K. D. M.; Bruce, P. G. Determination of a molecular crystal structure by X-ray powder diffraction on a conventional laboratory instrument. *J. Chem. Soc. Chem. Commun.* **1992**, 1012-1013.

(14) Harris, K. D. M.; Tremayne, M.; Lightfoot, P.; Bruce, P. G. Crystal structure determination from powder diffraction data by Monte Carlo methods. *J. Am. Chem. Soc.* **1994**, *116*, 3543-3547.

(15) Harris, K. D. M.; Habershon, S.; Cheung, E. Y.; Johnston, R. L. Developments in genetic algorithm techniques for structure solution from powder diffraction data. *Z. Kristallogr.* **2004**, *219*, 838-846.

(16) Tsue, H.; Horiguchi, M.; Tamura, R.; Fujii, K.; Uekusa, H. Crystal structure solution of organic compounds from X-ray powder diffraction data. *J. Synth. Org. Chem. Jpn.* **2007**, *65*, 1203-1212.

(17) David, W. I. F.; Shankland, K. Structure determination from powder diffraction data. *Acta Crystallogr. Sect. A.* **2008**, *64*, 52-64.

(18) Harris, K. D. M. Powder diffraction crystallography of molecular solids. *Top. Curr. Chem.* **2012**, *315*, 133-178.

(19) Martí-Rujas, J. Structural elucidation of microcrystalline MOFs from powder X-ray diffraction. *Dalton Trans.* **2020**, *49*, 13897-13916.

(20) Dudenko, D. V.; Williams, P. A.; Hughes, C. E.; Antzutkin, O. N.; Velaga, S. P.; Brown, S. P.; Harris, K. D. M. Exploiting the synergy of powder X-ray diffraction and solid-state NMR spectroscopy in structure determination of organic molecular solids. *J. Phys. Chem. C* **2013**, *117*, 12258-12265.

(21) Watts, A. E.; Maruyoshi, K.; Hughes, C. E.; Brown, S. P.; Harris, K. D. M. Combining the advantages of powder X-ray diffraction and NMR crystallography in structure determination of the pharmaceutical material cimetidine hydrochloride. *Cryst. Growth. Des.* **2016**, *16*, 1798-1804.

(22) Hughes, C. E.; Reddy, G. N. M.; Masiero, S.; Brown, S. P.; Williams, P. A.; Harris, K. D. M. Determination of a complex crystal structure in the absence of single crystals: analysis of powder X-ray diffraction data, guided by solid-state NMR and periodic DFT calculations, reveals a new 2'-deoxyguanosine structural motif. *Chem. Sci.* **2017**, *8*, 3971-3979.

(23) Delori, A.; Friščić, T.; Jones, W. The role of mechanochemistry and supramolecular design in the development of pharmaceutical materials. *CrystEngComm* **2012**, *14*, 2350-2362.

(24) James, S. L.; Adams, C. J.; Bolm, C.; Braga, D.; Collier, P.; Friščić, T.; Grepioni, F.; Harris, K. D. M.; Hyett, G.; Jones, W.; Krebs, A.; Mack, J.; Maini, L.; Orpen, A. G.; Parkin, I. P.; Shearouse, W. C.; Steed, J. W.; Waddell, D. C. Mechanochemistry: Opportunities for new and cleaner synthesis. *Chem. Soc. Rev.* **2012**, *41*, 413-447.

(25) Do, J.-L.; Friščić, T. Mechanochemistry: A force of synthesis. *ACS Cent. Sci.* **2017**, *3*, 13-19.

(26) Brown, G. R.; Caira, M. R.; Nassimbeni, L. R.; van Oudtshoorn, B. Inclusion of ibuprofen by heptakis(2,3,6-tri-O-methyl)-β-cyclodextrin: An X-ray diffraction and thermal analysis study. *J. Inclusion Phenom. Molec. Recogn. Chem.* **1996**, *26*, 281-294.

(27) Walsh, R. D. B.; Bradner, M. W.; Fleischman, S.; Morales, L. A.; Moulton, B.; Rodriguez-Hornedo, N.; Zaworotko, M. J. Crystal engineering of the composition of pharmaceutical phases. *Chem. Commun.* **2003**, 186-187.

(28) Berry, D. J.; Seaton, C. C.; Clegg, W.; Harrington, R.W.; Coles, S.J.; Horton, P.N.; Hursthouse, M.B.; Storey, R.; Jones, W.; Friščić, T.; Blagden, N. Applying hot-stage microscopy to co-crystal screening: A study of nicotinamide with seven active pharmaceutical ingredients. *Cryst. Growth Des.* **2008**, *8*, 1697-1712.

(29) Molnar, P.; Bombicz, P.; Varga, C.; Bereczki, L.; Szekely, E.; Pokol, G.; Fogassy, E.; Simandi, B. Influence of benzylamine on the resolution of ibuprofen with (+)-(R)-phenylethylamine via supercritical fluid extraction. *Chirality*, **2009**, *21*, 628-636.

(30) Chen, S.; Xi, H.; Henry, R. F.; Marsden, I.; Zhang, G. G. Z. Chiral co-crystal solid solution: structures, melting point phase diagram, and chiral enrichment of (ibuprofen)$_2$(4,4-dipyridyl). *CrystEngComm*, **2010**, *12*, 1485-1493.

(31) Alshahateet, S. F. Synthesis and supramolecularity of hydrogen-bonded cocrystals of pharmaceutical model rac-ibuprofen with pyridine derivatives. *Mol. Cryst. Liquid Cryst.*, **2010**, *533*, 152-161.

(32) Alshahateet, S. F. Synthesis and X-ray crystallographic analysis of pharmaceutical model rac-ibuprofen cocrystal. *J. Chem. Crystallogr.* **2011**, *41*, 276-279.

(33) Springuel, G.; Robeyns, K.; Norberg, B.; Wouters, J.; Leyssens, T. Cocrystal formation between chiral compounds: How cocrystals differ from salts. *Cryst. Growth Des.* **2014**, *14*, 3996-4004.

(34) Deshpande, P. P. *et al.* A practical stereoselective synthesis and novel cocrystallizations of an amphiphatic SGLT-2 inhibitor. *Org. Process Res. Dev.* **2012**, *16*, 577-585.

(35) We note that the level of hydration of the different samples (prepared under different conditions) that exhibit the powder XRD pattern characteristic of **Ibu-Pro-QH** has not been

explored. Preliminary studies of dehydration of **Ibu-Pro-QH** discussed in Section 3.7 suggest that, upon dehydration at 77 °C, the powder XRD pattern is essentially the same as that of fully hydrated **Ibu-Pro-QH**. Thus, it is possible that samples obtained under different conditions, all of which give the powder XRD pattern characteristic of **Ibu-Pro-QH**, could have different levels of hydration up to a maximum corresponding to the quarter-hydrate.

(36) Metz, G.; Wu, X. L.; Smith, S. O. Ramped-amplitude cross polarization in magic-angle-spinning NMR. *J. Magn. Reson. A* **1994**, *110*, 219-227.

(37) Fung, B. M.; Khitrin, A. K.; Ermolaev, K. An improved broadband decoupling sequence for liquid crystals and solids. *J. Magn. Reson.* **2000**, *142*, 97-101.

(38) Clark, S. J.; Segall, M. D.; Pickard, C. J.; Hasnip, P. J.; Probert, M. J.; Refson, K.; Payne, M. C. First principles methods using CASTEP. *Z. Kristallogr.* **2005**, *220*, 567-570.

(39) Vanderbilt, D. Soft self-consistent pseudopotentials in a generalized eigenvalue formalism. *Phys. Rev. B* **1990**, *41*, 7892-7895.

(40) Perdew, J. P.; Burke, K.; Ernzerhof, M. Generalized gradient approximation made simple. *Phys. Rev. Lett.* **1996**, *77*, 3865-3868.

(41) Tkatchenko, A.; Scheffler, M. Accurate molecular Van Der Waals interactions from ground-state electron density and free-atom reference data. *Phys. Rev. Lett.* **2009**, *102*, 073005.

(42) Monkhorst, H. J.; Pack, J. D. Special points for Brillouin-zone integrations. *Phys. Rev. B* **1976**, *13*, 5188-5192.

(43) We recall that the molecular symmetry for an individual (*S*)-ibuprofen molecule is C1. Thus, the (*S*)-ibuprofen molecule(s) cannot be located on a crystallographic symmetry element and must therefore occupy a general position in the crystal structure.

(44) Cheung, E. Y.; Kitchin, S. J.; Harris, K. D. M.; Imai, Y.; Tajima, N.; Kuroda, R. Direct structure determination of a multicomponent molecular crystal prepared by a solid-state grinding procedure. *J. Am. Chem. Soc.* **2003**, *125*, 14658–14659.

(45) Fujii, K.; Garay, A. L.; Hill, J.; Sbircea, E.; Pan, Z.; Xu, M.; Apperley, D. C.; James, S. L.; Harris, K. D. M. Direct structure elucidation by powder X-ray diffraction of a metal-organic framework material prepared by solvent-free grinding. *Chem. Commun.* **2010**, *46*, 7572-7574.

(46) Ma, X.; Lim, G. K.; Harris, K. D. M.; Apperley, D. C.; Horton, P. N.; Hursthouse, M. B.; James, S. L. Efficient, scalable and solvent-free mechanochemical synthesis of the OLED material Alq_3 (q = 8-hydroxyquinolinate). *Cryst. Growth. Des.* **2012**, *12*, 5869-5872.

(47) Zhou, Y.; Guo, F.; Hughes, C. E.; Browne, D. L.; Peskett, T. R.; Harris, K. D. M. Discovery of new meta-stable polymorphs in a family of urea co-crystals by solid-state mechanochemistry. *Cryst. Growth. Des.* **2015**, *15*, 2901-2907.

(48) Al Rahal, O.; Majumder, M.; Spillman, M. J.; van de Streek, J.; Shankland, K. Co-crystal structures of furosemide:urea and carbamazepine:indomethacin determined from powder X-ray diffraction data. *Crystals.* **2020**, *10*, 42.

(49) Brekalo, I.; Yuan, W.; Mottillo, C.; Lu, Y.; Zhang, Y.; Casaban, J.; Holman, K. T.; James, S. L.; Duarte, F.; Williams, P. A.; Harris, K. D. M.; Friščić, T. Manometric real-time studies of the mechanochemical synthesis of zeolitic imidazolate frameworks. *Chem. Sci.* **2020**, *11*, 2141-2147.

(50) Werner, P.-E.; Eriksson, L.; Westdahl, M. TREOR, a semi-exhaustive trial-and-error powder indexing program for all symmetries. *J. Appl. Cryst.* **1985**, *18*, 367-370.

(51) Shirley, R. The CRYSFIRE 2002 System for Automatic Powder Indexing: User's Manual, The Lattice Press, Guildford, Surrey, U.K., 2002.

(52) Le Bail, A.; Duroy, H.; Fourquet, J. L. Ab-initio structure determination of $LiSbWO_6$ by X-ray powder diffraction. *Mater. Res. Bull.* **1988**, *23*, 447-452.

(53) Larson, A. C.; Von Dreele, R. B. Los Alamos National Laboratory Report 2004, LAUR 86-748.

(54) Albesa-Jové, D.; Kariuki, B. M.; Kitchin, S. J.; Grice, L.; Cheung, E. Y.; Harris, K. D. M. Challenges in direct-space structure determination from powder diffraction data: A molecular material with four independent molecules in the asymmetric unit. *ChemPhysChem.* **2004**, *5*, 414-418.

(55) Guo, F.; Martí-Rujas, J.; Pan, Z.; Hughes, C. E.; Harris, K. D. M. Direct structural understanding of a topochemical solid state photopolymerization reaction. *J. Phys. Chem. C* **2008**, *112*, 19793-19796.

(56) Courvoisier, E.; Williams, P. A.; Lim, G. K.; Hughes, C. E.; Harris, K. D. M. The crystal structure of L-arginine. *Chem. Commun.* **2012**, *48*, 2761-2763.

(57) Williams, P. A.; Hughes, C. E.; Lim, G. K.; Kariuki, B. M.; Harris, K. D. M. Discovery of a new system exhibiting abundant polymorphism: *m*-aminobenzoic acid. *Cryst. Growth. Des.* **2012**, *12*, 3104-3113.

(58) Martí-Rujas, J.; Meazza, L.; Lim, G. K.; Terraneo, G.; Pilati, T.; Harris, K. D. M.; Metrangolo, P.; Resnati, G. An adaptable and dynamically porous organic salt traps unique tetrahalide dianions. *Angew. Chem. Int. Ed.* **2013**, *52*, 13444-13448.

(59) Williams, P. A.; Hughes, C. E.; Harris, K. D. M. L-Lysine: exploiting powder X-ray diffraction to complete the set of crystal structures of the 20 directly-encoded proteinogenic amino acids. *Angew. Chem. Int. Ed.* **2015**, *54*, 3973-3977.

(60) Al Rahal, O.; Hughes, C. E.; Williams, P. A.; Logsdail, A. J.; Diskin-Posner, Y.; Harris, K. D. M. Polymorphism of L-tryptophan. *Angew. Chem. Int. Ed.* **2019**, *58*, 18788-18792.

(61) Kayushina, R. L.; Vainshtein, B. K. X-ray determination of structure of L-proline. *Kristallografiya* **1965**, *10*, 833-844.

(62) Following structure solution, the conformation of the ring in the L-proline molecule was allowed to relax in subsequent stages of the structure determination process, both in Rietveld refinement and in DFT-D geometry optimization calculations.

(63) Bruno, I. J.; Cole, J. C.; Kessler, M.; Luo, J.; Motherwell, W. D. S.; Purkis, L. H.; Smith, B. R.; Taylor, R.; Cooper, R. I.; Harris, S. E.; Orpen, A. G. Retrieval of crystallographically-derived molecular geometry information. *J. Chem. Inf. Comput. Sci.* **2004**, *44*, 2133-2144.

(64) Allen, F. H.; Kennard, O.; Watson, D. G.; Brammer, L.; Orpen, A. G.; Taylor, R. Tables of bond lengths determined by X-ray and neutron diffraction. Part 1. Bond lengths in organic compounds. *J. Chem. Soc. Perkin Trans. 2* **1987**, S1-S19.

(65) With the exception that, for **Ibu-Pro-QH**, a common isotropic displacement parameter was refined for the non-hydrogen atoms in the two molecules of (*S*)-ibuprofen, the two molecules of L-proline and the water molecule.

(66) We note that the measured unit cell volume at 77 °C may be lower than that for fully hydrated **Ibu-Pro-QH** if partial dehydration occurred during heating from ambient temperature to 77 °C.

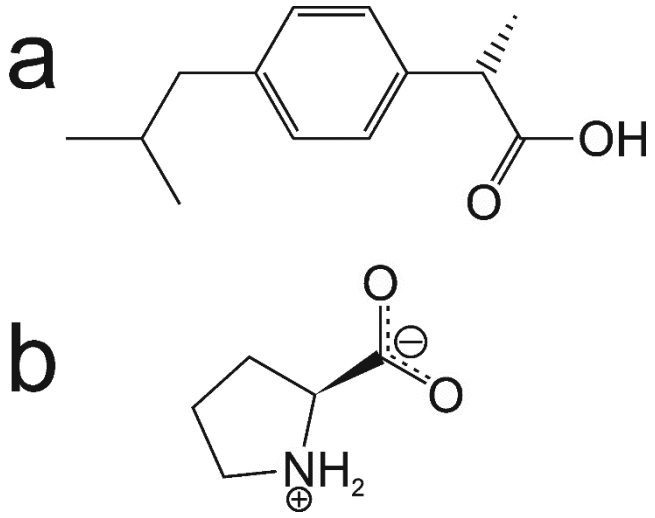

Figure 1. Molecular structures of (a) (*S*)-ibuprofen and (b) L-proline. The stereochemistry of the chiral centre in each molecule is indicated.

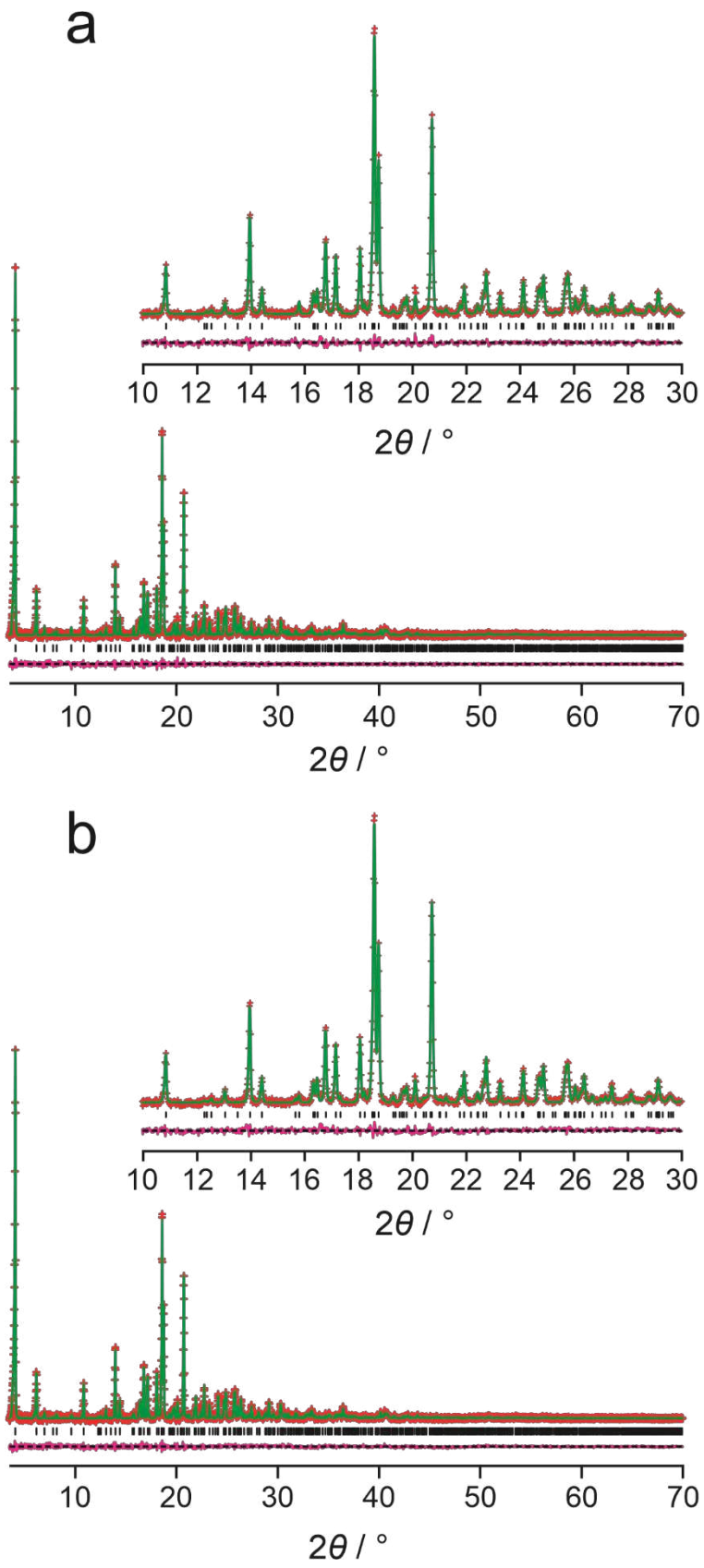

Figure 2. (a) Le Bail fit and (b) final Rietveld refinement for **Ibu-Pro** (red crosses, experimental data following background subtraction; green line, calculated data; magenta line, difference plot; black tick marks, predicted peak positions).

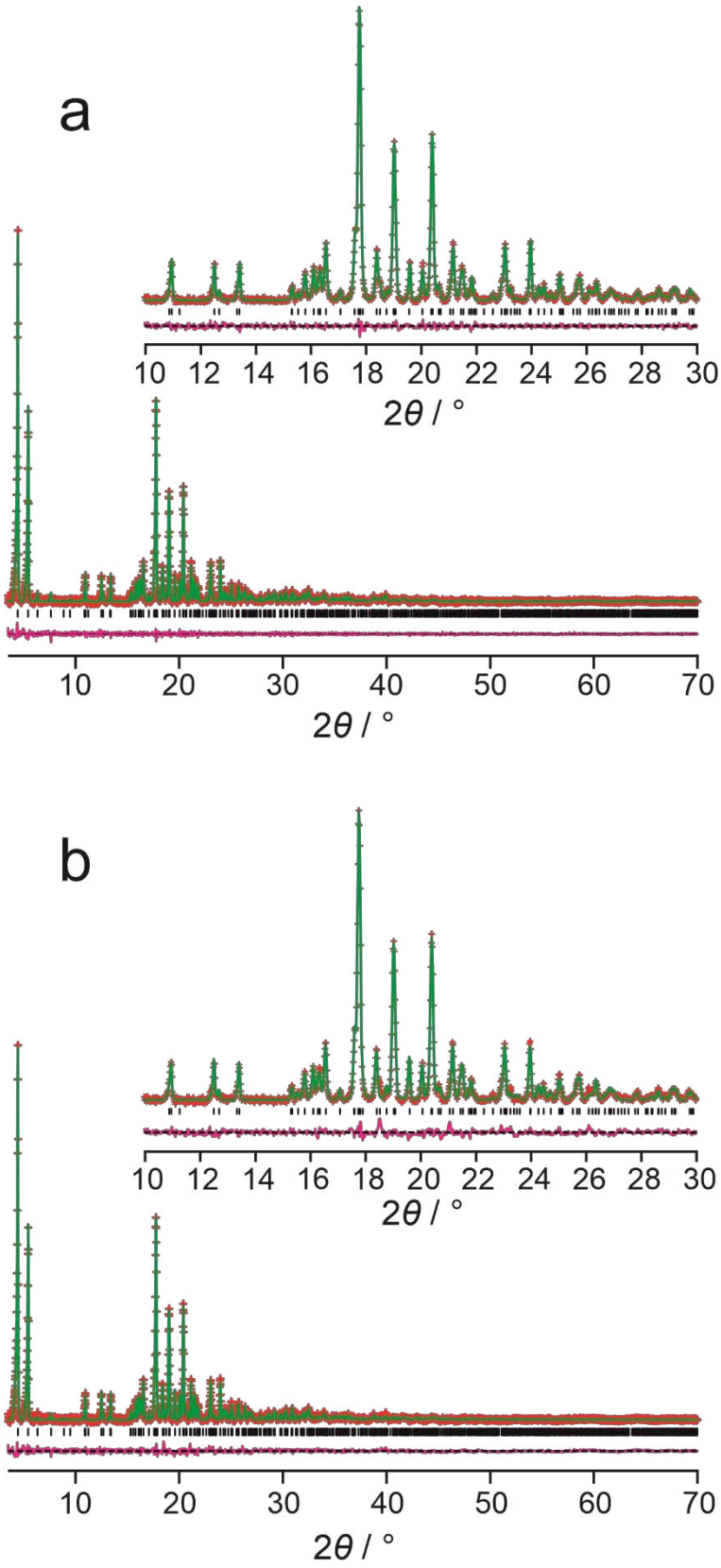

Figure 3. (a) Le Bail fit and (b) final Rietveld refinement for **Ibu-Pro-QH** (red crosses, experimental data following background subtraction; green line, calculated data; magenta line, difference plot; black tick marks, predicted peak positions).

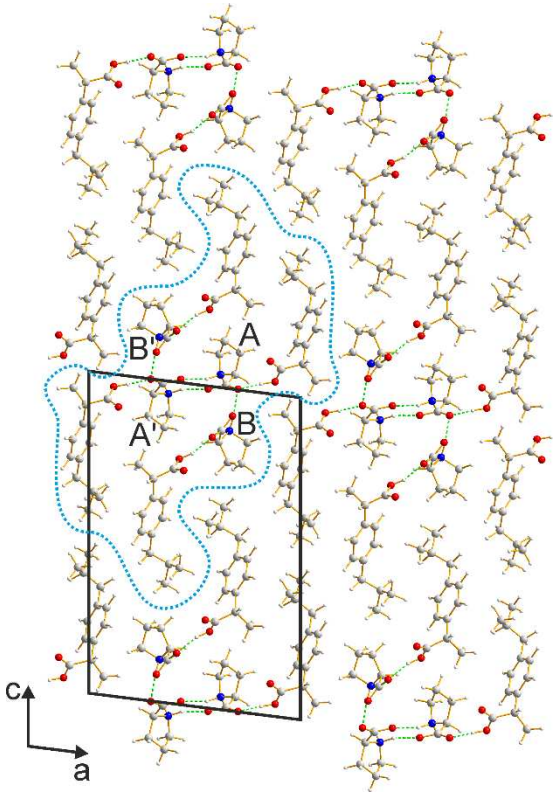

Figure 4. Crystal structure of **Ibu-Pro** viewed along the *b*-axis. Hydrogen bonds are indicated by green dashed lines. The two independent L-proline molecules are labelled A and B, and the L-proline molecules related to these molecules by the 2_1-screw axis are labelled A' and B', respectively. The region defined by the blue dotted line contains an A-A' hydrogen-bonded L-proline ribbon, an A-B hydrogen-bonded L-proline ribbon (and the symmetry-related A'-B' hydrogen-bonded L-proline ribbon), and the (*S*)-ibuprofen molecules linked by hydrogen-bonding to the periphery of the L-proline ribbons.

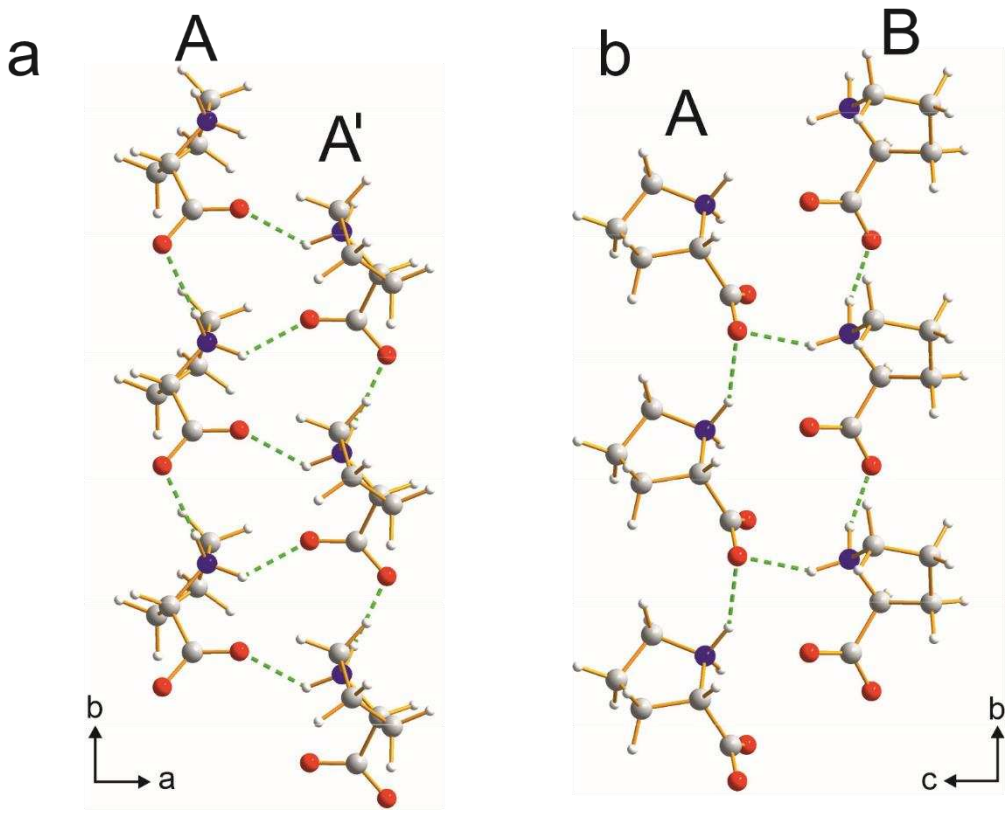

Figure 5. The hydrogen-bonded ribbons of L-proline molecules in **Ibu-Pro**: (a) the A-A' ribbon, and (b) the A-B ribbon. Green dashed lines indicate hydrogen bonding.

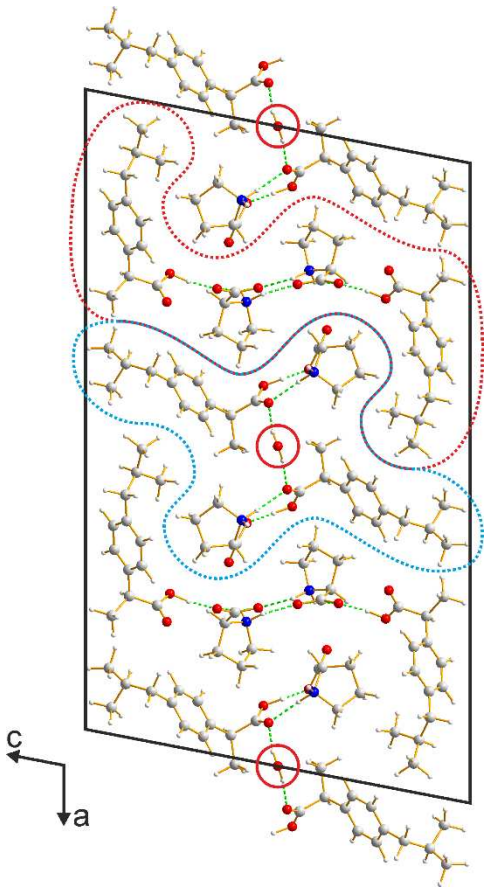

Figure 6. Crystal structure of **Ibu-Pro-QH** viewed along the *b*-axis. The two hydrogen-bonded regions are indicated by the blue dotted line (region W) and the red dotted line (region N). Hydrogen bonds are indicated by green dashed lines. The water molecule (highlighted by the red circle) is located on a 2-fold rotation axis parallel to the *b*-axis.

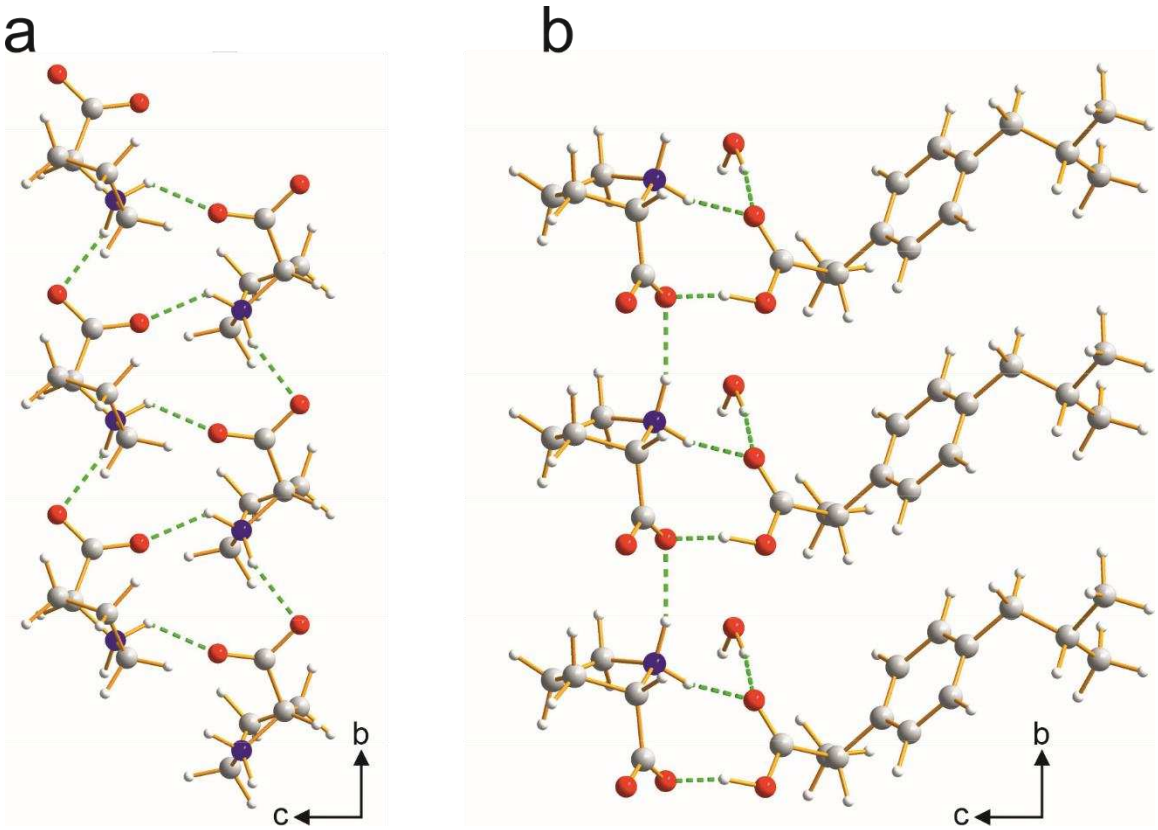

Figure 7. Hydrogen-bonding arrangements in **Ibu-Pro-QH**: (a) the hydrogen-bonded ribbon of L-proline molecules in region N [the (*S*)-ibuprofen molecules that link to the periphery of this ribbon are not shown], and (b) the symmetry independent part of the hydrogen-bonding arrangement in region W (the complete hydrogen-bonding arrangement is generated by the 2-fold rotation axis parallel to the *b*-axis, which is coincident with the molecular 2-fold axis of the water molecule).

For Table of Contents Use Only

Structure determination of multicomponent crystalline phases of (*S*)-ibuprofen and L-proline from powder X-ray diffraction data, augmented by complementary experimental and computational techniques

Okba Al Rahal, P. Andrew Williams, Colan E. Hughes, Benson M. Kariuki, Kenneth D. M. Harris*

TOC Graphic

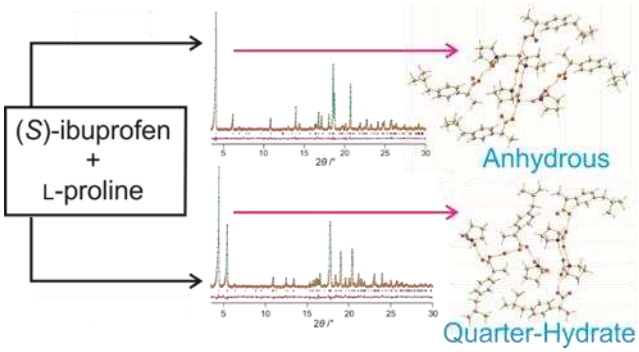

Synopsis

Two multicomponent crystalline phases containing (*S*)-ibuprofen and L-proline in 1:1 stoichiometry are reported, specifically a non-solvate and a quarter-hydrate. The structural properties of each phase were determined from powder XRD data using the direct-space strategy for structure solution followed by Rietveld refinement. The structure determination process was augmented by information from solid-state NMR, thermal analysis and periodic DFT-D calculations.